

Autonomous Navigation and Map building Using Laser Range Sensors in Outdoor Applications

Jose Guivant, Eduardo Nebot and Stephan Baiker

Australian Centre for Field Robotics
Department of Mechanical and Mechatronic Engineering
The University of Sydney, NSW 2006, Australia
jguivant/nebot @mech.eng.usyd.edu.au

Abstract

This paper presents the design of a high accuracy outdoor navigation system based on standard dead reckoning sensors and laser range and bearing information. The data validation problem is addressed using laser intensity information. The beacon design aspect and location of landmarks are also discussed in relation to desired accuracy and required area of operation. The results are important for Simultaneous Localization and Map building applications, (SLAM), since the feature extraction and validation are resolved at the sensor level using laser intensity. This facilitates the use of additional natural landmarks to improve the accuracy of the localization algorithm. The modelling aspects to implement SLAM with beacons and natural features are also presented. These results are of fundamental importance because the implementation of the algorithm does not require the surveying of beacons. Furthermore we demonstrate that by using natural landmarks high accurate localization can be achieved by only requiring the initial estimate of the position of the vehicle. The algorithms are validated in outdoor environments using a standard utility car retrofitted with the navigation sensors and a 1 cm precision Kinematic GPS used as ground truth.

1 Introduction

Reliable localization is an essential component of any autonomous vehicle. The basic navigation loop is based on dead reckoning sensors that predict the vehicle high frequency manoeuvres and low frequency absolute sensors that bound the positioning errors [1].

For almost every land navigation application we can always find an appropriate combination of dead reckoning sensors that can be used to obtain a reasonable prediction of the trajectory of the vehicle, [2],[3]. With external sensors the problem is more complicated. Although there are many different types of external sensors, only few of them can be used in a particular application and the reliability will be function of the environment of operation, [4].

It is well known that with the different GPS implementations, position fixes with errors of the order of 1 cm. to 100 m. can be obtained in real time. Nevertheless this accuracy cannot be guarantee all the time in most working environments where partial satellite occlusion and multipath effects can prevent normal GPS receiver operation. Similar problems are experienced with some other type of sensors such as Stereo Vision, Ultrasonic, Laser and Radars.

A significant amount of work has been devoted to the use of range and bearing sensors for localization purposes. Ultrasonic sensors have been widely used in indoor applications [5], but they are not adequate for most outdoor applications due to range limitations and bearing uncertainties.

Stereovision has been the object of research in many important research laboratories around the world. Recently in [6], stereoscopic omni directional systems were used in indoor localization applications. This type of sensor is based on a conical mirror and a camera that returns a panoramic image of the environment surrounding the vehicle. Although a promising technology, the complexity and its poor dynamic range made this technique still not very reliable for outdoor applications.

Millimeter Wave Radar [7], is an emerging technology that has enormous potential for obstacle detection, map building and navigation in indoor and outdoor applications. The main drawback of this technology is its actual cost but this is expected to change in the near future. Millimeter Wave Radar had been used for localization purposes in [8] and in SLAM applications in [9]. In this case, special beacons were designed to increase the echo return intensity such that simple threshold or more sophisticated polarization techniques can be used to discriminate beacons from background at the sensor level.

Range and bearing lasers have become one of the most attractive sensors for localization and map building purposes due to their accuracy and low cost. Most common lasers provide range and bearing information with sub degree resolution and accuracies of the order of 1-10 cm in 10-50 meter ranges.

There are a number of works that addressed the localization using pose information [10], [11]. These works update the position of the vehicle based on the determination of the transformation between the pose of the robot and the laser measurements. Laser has also been used to determine natural features in indoor environments. In [12] a comparison of the behaviour monocular, trinocular and laser in localization applications is presented.

One of the most difficult problems for any beacon localization based algorithm is not feature extraction, but feature validation and data association. That is to confirm that the extracted feature is a valid feature and to associate it with a known or estimated feature in the world map. Data association is essential for the SLAM problem. This problem has been addressed in previous works using redundant information by looking for stable features [9] or using a combination of sensors such as in [13], where vision information is used to validate certain type of features extracted from laser information.

This work makes use of laser intensity information to recognize landmarks. It presents the characterization of the laser and design issues for landmark detection using this type of laser. It demonstrates that high accurate localization can be obtained with this information. A full SLAM implementation using beacon and beacons and natural features is presented. Analysis of absolute and relative errors are also discussed. The navigation algorithm is implemented in information form. This algorithm becomes more attractive than the standard Kalman filter for application where the external information is available from different sources and at different times [1].

This paper begins in Section 2 by describing the modelling aspects of the navigation loop and the extension to SLAM. The characterization of the sensor is presented in Section 3 and the information filter in Section 4. Finally Section 5 and 6 present the experimental results and conclusions

2 Navigation loop

The navigation loop is based on encoders and range/ bearing information provided by a laser sensor. The models for the process and observation are non-linear. The encoders provide velocity and steering angle information that is used with a kinematic model of the vehicle to predict position and orientation. The prediction is updated with external range and bearing information provided by a laser sensor.

Modelling Aspect

A simple kinematic model is used for this experimentation. This model can be extended to consider other parameters such as wheel radius and slip angle that can have significant importance in other applications [3].

The vehicle position is represented in global coordinates as shown in Figure 1 . The steering control α is defined in vehicle coordinate frame. The laser sensor is located in the front of the vehicle and returns range and bearing related to objects at distances of up to 50 meters. High intensity reflection can be obtained by placing high reflectivity beacons in the area of operation. These landmarks are labelled as $Bi_{(i=1..n)}$ and measured with respect to the vehicle coordinates (x_1, y_1) , that is $z(k) = (r, \beta, I)$, where r is the distance from the beacon to the laser, β is the sensor bearing measured with respect to the vehicle coordinate frame and I is the intensity information.

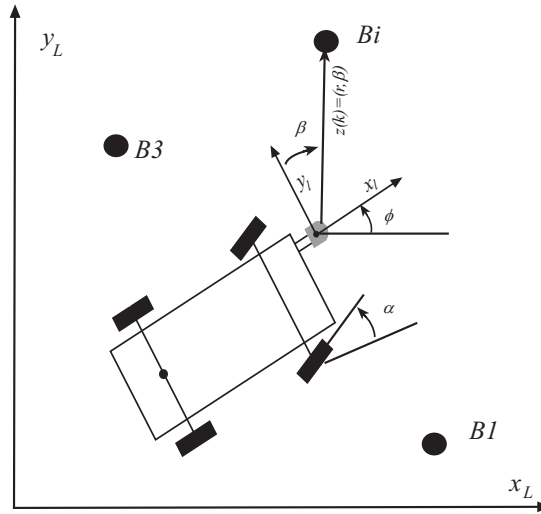


Figure 1 Vehicle coordinate system

Considering that the vehicle is controlled through a demanded velocity v_c and steering angle α the process model that predict the trajectory of the centre of the back axle is given by

$$\begin{bmatrix} \dot{x}_c \\ \dot{y}_c \\ \dot{\phi}_c \end{bmatrix} = \begin{bmatrix} v_c \cdot \cos(\phi) \\ v_c \cdot \sin(\phi) \\ \frac{v_c}{L} \cdot \tan(\alpha) \end{bmatrix} \quad (1)$$

The laser is located in the front of the vehicle. To facilitate the update stage, the kinematic model of the vehicle is designed to represent the trajectory of the centre of the laser. Based on Figure 1 and 2 , the translation of the centre of the back axle can be given

$$P_L = P_C + a \cdot \vec{T}_\phi + b \cdot \vec{T}_{\phi + \pi/2} \quad (2)$$

Being P_L and P_C the position of the laser and the centre of the back axle in global coordinates. The transformation is defined by the orientation angle, according to the following vectorial expression:

$$\vec{T}_\phi = (\cos(\phi), \sin(\phi)) \quad (3)$$

The scalar representation is

$$\begin{aligned} x_L &= x_c + a \cdot \cos(\phi) + b \cdot \cos\left(\phi + \frac{\pi}{2}\right) \\ y_L &= y_c + a \cdot \sin(\phi) + b \cdot \sin\left(\phi + \frac{\pi}{2}\right) \end{aligned} \quad (4)$$

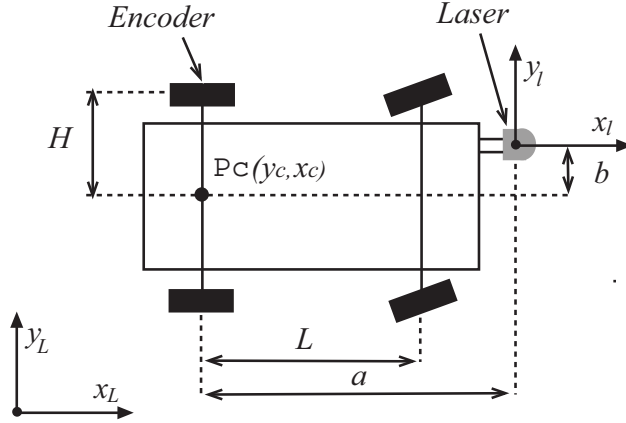


Figure 2 Kinematics parameters

Finally the full state representation can be written

$$\begin{bmatrix} \dot{x}_L \\ \dot{y}_L \\ \dot{\phi}_L \end{bmatrix} = \begin{bmatrix} v_c \cdot \cos(\phi) - \frac{v_c}{L} \cdot (a \cdot \sin(\phi) + b \cdot \cos(\phi)) \cdot \tan(\alpha) \\ v_c \cdot \sin(\phi) + \frac{v_c}{L} \cdot (a \cdot \cos(\phi) - b \cdot \sin(\phi)) \cdot \tan(\alpha) \\ \frac{v_c}{L} \cdot \tan(\alpha) \end{bmatrix} \quad (5)$$

The velocity is generated with an encoder located in the back left wheel. This velocity is translated to the centre of the axle with the following equation:

$$v_c = \frac{v_e}{\left(1 - \tan(\alpha) \cdot \frac{H}{L}\right)} \quad (6)$$

Where for this car $H = 0.75\text{m}$, $L = 2.83\text{ m}$, $b = 0.5$ and $a = L + 0.95\text{m}$. Finally the discrete model in global coordinates can be approximated with the following set of equations:

$$\begin{bmatrix} x(k) \\ y(k) \\ \phi(k) \end{bmatrix} = \begin{bmatrix} x(k-1) + \Delta t v_c(k-1) \cdot \cos(\phi(k-1)) - \\ \frac{v_c}{L} \cdot (a \cdot \sin(\phi(k-1)) + b \cdot \cos(\phi(k-1))) \\ \cdot \tan(\alpha(k-1)) \\ y(k-1) + \Delta t v_c(k-1) \cdot \sin(\phi(k-1)) + \\ \frac{v_c(k-1)}{L} \cdot (a \cdot \cos(\phi(k-1)) - b \cdot \sin(\phi(k-1))) \\ \cdot \tan(\alpha(k-1)) \\ \frac{v_c(k-1)}{L} \cdot \tan(\alpha(k-1)) \end{bmatrix} \quad (7)$$

where ΔT is the sampling time, that in our case is not constant. The process can then be written as a nonlinear equation

$$\begin{aligned} X(k) &= f(X(k-1), u(k-1) + \mu(k-1)) + \omega_f(k-1) \\ X(k) &\approx f(X(k-1), u(k-1)) + \omega_u(k-1) + \omega_f(k-1) \end{aligned} \quad (8)$$

where $X(k-1)$ and $u(k-1)$ are the estimate and input at time $k-1$ and $\mu(k-1)$ and $\omega_f(k-1)$ are process noises. The process noise is mainly due to measurements error in the velocity and steering input information. The model for $\omega_u(k)$ is given by:

$$[\omega_u(k)] = [\nabla f_{u(k-1)}(X, u)] \cdot \mu(k) \quad (9)$$

where $\nabla f_u = \frac{\partial f}{\partial u} = \frac{\partial(x, y, \phi)}{\partial(u_1, u_2)}$ is the gradient of f with respect to the input $u = (u_1, u_2) = (v, \alpha)$ and $\mu(k)$ is Gaussian noise.

The equation that relates the observation with the states is

$$\begin{bmatrix} z_r^i \\ z_\beta^i \end{bmatrix} = h(X, x_i, y_i) = \begin{bmatrix} \sqrt{(x_L - x_i)^2 + (y_L - y_i)^2} \\ \text{atan}\left(\frac{(y_L - y_i)}{(x_L - x_i)}\right) - \phi + \pi/2 \end{bmatrix} \quad (10)$$

where z and $[x, y, \phi]$ are the observation and state values respectively, and (x_i, y_i) are the positions of the beacons or natural landmarks. The observation equation can be expressed in short form as

$$z(k) = h(x(k)) + \eta(k) \quad (11)$$

with

$$\eta(k) = \begin{bmatrix} \eta_R(k) \\ \eta_\beta(k) \end{bmatrix} \quad (12)$$

The noises $\mu(k)$ and $\eta(k)$ are assumed to be Gaussian, temporally uncorrelated and zero mean, that is

$$E[\mu(k)] = E[\eta(k)] = 0 \quad (13)$$

with corresponding covariance

$$E[\mu(i)\mu^T(j)] = \delta_{ij} Q_{\alpha, v}(i), \quad E[\eta(i)\eta^T(j)] = \delta_{ij} R_{r, \beta}(i) \quad (14)$$

Simultaneous Localization and Map Building

The localization and map building problem can also be approached with this combination of sensors. In this case the estimated location of the features or beacon becomes part of the state vector. The vehicle start at an unknown position with a given uncertainty and obtain measurements of the environment relative to its position. This information is used to incrementally build and maintain a navigation map and localize with respect to this map.

The state vector is now given by:

$$\begin{aligned}
X &= \begin{bmatrix} x_v \\ x_L \end{bmatrix} \\
x_v &= (x, y, \phi) \in \mathbb{R}^3 \\
x_L &= (x_1, y_1, \dots, x_n, y_n) \in \mathbb{R}^N
\end{aligned} \tag{15}$$

where x_v and x_L are the states of the vehicle and actual landmarks. The landmarks can be natural features of special designed beacon located at unknown location. The dynamic model of the extended system that considers the new states can now be written:

$$\begin{aligned}
x_v(k+1) &= f(x_v(k)) \\
x_L(k+1) &= x_L(k)
\end{aligned} \tag{16}$$

It can be seen that the dynamic of the states x_L is invariant since the landmarks are assumed to be static.

Then the Jacobian matrix for the extended system becomes

$$\frac{\partial F}{\partial X} = \begin{bmatrix} \frac{\partial f}{\partial x_v} & \emptyset \\ \emptyset^T & I \end{bmatrix} = \begin{bmatrix} J_1 & \emptyset \\ \emptyset^T & I \end{bmatrix} \tag{17}$$

$$J_1 \in \mathbb{R}^{3 \times 3}, \quad \emptyset \in \mathbb{R}^{3 \times N}, \quad I \in \mathbb{R}^{N \times N}$$

The observations obtained with a range and bearing device are relative to the vehicle position. The observation equation is a function of the state of the vehicle and the states representing the position of the landmark:

$$\begin{aligned}
r_i = h_r(X) &= \|(x, y) - (x_i, y_i)\|_2 = \sqrt{(x - x_i)^2 + (y - y_i)^2} \\
\alpha_i = h_\alpha(X) &= \text{atan} \left(\frac{(y - y_i)}{(x - x_i)} \right) - \phi + \frac{\pi}{2}
\end{aligned} \tag{18}$$

where (x, y) is the position of the vehicle, (x_i, y_i) the position of the landmark numbered i and ϕ the orientation of the car.

Then the Jacobian matrix of the vector (r_i, α_i) respect to the variables (x, y, ϕ, x_i, y_i) can be evaluated using:

$$\frac{\partial h}{\partial X} = \begin{bmatrix} \frac{\partial h_r}{\partial X} \\ \frac{\partial h_\alpha}{\partial X} \end{bmatrix} = \begin{bmatrix} \frac{\partial r_i}{\partial(x, y, \phi, \{x_i, y_i\})} \\ \frac{\partial \alpha_i}{\partial(x, y, \phi, \{x_i, y_i\})} \end{bmatrix} \tag{19}$$

with

$$\frac{\partial h_r}{\partial X} = \frac{1}{\Delta} \cdot [\Delta x, \Delta y, 0, 0, 0, \dots, -\Delta x, -\Delta y, 0, \dots, 0, 0]$$

$$\frac{\partial h_\alpha}{\partial X} = \left[-\frac{\Delta y}{\Delta^2}, \frac{\Delta x}{\Delta^2}, -1, 0, 0, \dots, \frac{\Delta y}{\Delta^2}, -\frac{\Delta x}{\Delta^2}, 0, \dots, 0, 0 \right] \quad (20)$$

$$\Delta x = (x - x_i), \quad \Delta y = (y - y_i), \quad \Delta = \sqrt{(\Delta x)^2 + (\Delta y)^2}$$

These equations can be used to build and maintain a navigation map of the environment and to track the position of the vehicle.

3 Range/Bearing/Intensity laser information

This section presents the description of the laser and the beacon design aspects. The laser used in this experiment is the LMS200 model manufactured by SICK. It can return up to 361 range values spaced 0.5 degrees. The current version returns intensity information with eight different levels of magnitude. This information is used to detect beacons. The laser returns intensity information only from surfaces with high reflectivity. This information is extremely reliable and becomes of fundamental importance for navigation purposes.

The beacon design is of fundamental importance for the successful operation of the system. In a given area of operation, the accuracy of the navigation system will be a function of the size, shape and type of material of the reflector. In order to optimally design the reflector it is essential to characterize the laser beam. A set of experiments was designed to obtain the laser parameters. A retro reflective tape (1.5x15cm) was radially moved at a constant distance R in steps of 5mm perpendicular to the laser beam. The Intensity output of the scanner was recorder for different radius. The results corresponding to two different radius are shown in figures 3 and 4.

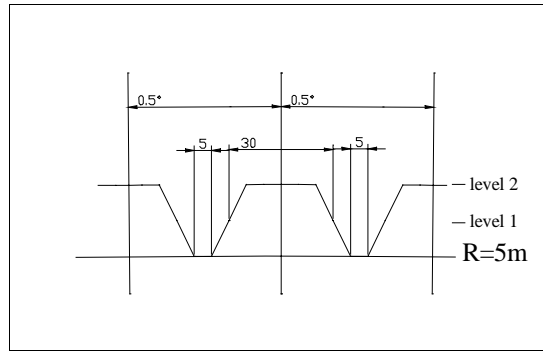


Figure 3. Intensity at 5m, beam $\varnothing \approx 30$ mm, shadow 5 mm (5mm reflector)

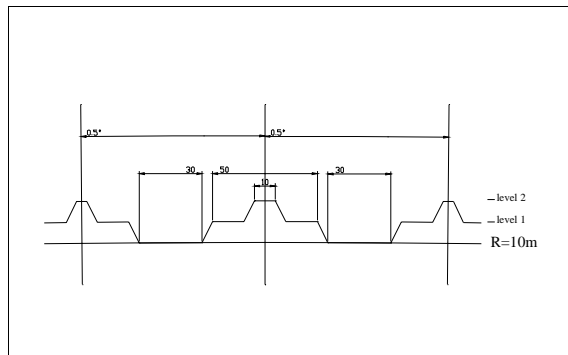


Figure 4. Intensity at 10m, beam $\varnothing \approx 50\text{mm}$, shadow 30 mm. (5mm reflector)

With this information the angular resolution of the scanner as well as the opening angle of the beam was evaluated. The characterization of the laser obtained is shown in Figure 5. The beam angle becomes approximately 0.2 degrees. This determines the minimum area of a beacon that will be able to return maximum intensity at a given distance.

In our experimentation we used standard diamond grade reflective tape. It was determined that the laser was able to detect beacons at distances of over 35 meters using reflectors with an area of 900 cm^2 .

The size and shape of the beacon also becomes important when high accuracy is required. One of the problem is that at short ranges the landmarks will be detected at different bearing angles.

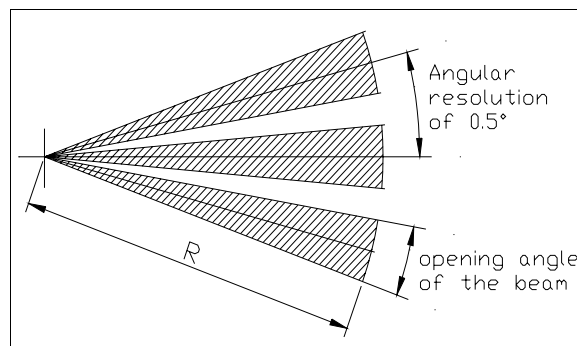


Figure 5 Laser Characteristics

This problem is shown in Figure 6 for a flat and cylindrical reflector. It can be seen that depending of the orientation and position of the vehicle the same beacon will be detected a different locations. The beacon shape is also of importance to be able to see the landmarks form different vehicle orientations. The cylinder shape shown in Figure 6 becomes very attractive for visibility purposes but it can generate different range and bearing returns depending on the position of the vehicle. These problems make the observation of the position of landmarks less accurately. Finally the “V” shape with an angle of 40 degrees provided the best results as trade-off between visibility and position determination. For each application the final selection of the shape and size of the landmarks will depend on the number of landmarks, the required accuracy and the area of operations in relation to the characteristic of the laser.

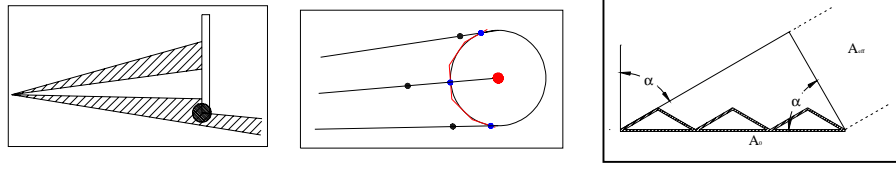


Figure 6 Different type of Beacons

This section presented the main characteristics of the laser scanner and addressed the beacon design problem. This information is essential to evaluate the maximum accuracy that can be obtained with this navigation system.

4 Information Filter

In this work we used the information Filter, also known as inverse covariance filter [1], to implement the navigation algorithm.

The information filter is a Kalman filter that expresses the optimal estimate in terms of the inverse of the covariance matrix

$$\mathbf{Y}(i | j) = \mathbf{P}^{-1}(i | j) \quad (21)$$

and the information state vector

$$\mathbf{y}(i | j) = \mathbf{P}^{-1}(i | j)\mathbf{x}(i | j). \quad (22)$$

Consider a linear system represented by

$$\mathbf{x}(k) = \mathbf{F}(k)\mathbf{x}(k-1) + \boldsymbol{\omega}(k), \quad (23)$$

where $\mathbf{x}(k)$ is the state vector at time k , $\mathbf{F}(k)$ is the state transition matrix and $\boldsymbol{\omega}(k)$ is a white process noise sequence with $\mathbf{E}[\boldsymbol{\omega}(i)\boldsymbol{\omega}^T(j)] = \delta_{ij}\mathbf{Q}(i)$. The observation is modelled as

$$\mathbf{z}(k) = \mathbf{H}(k)\mathbf{x}(k) + \boldsymbol{\eta}(k), \quad (24)$$

where $\mathbf{z}(k)$ is the observation vector, $\mathbf{H}(k)$ is the observation model and $\boldsymbol{\eta}(k)$ is a white observation (measurement) noise sequence with $\mathbf{E}[\boldsymbol{\eta}(i)\boldsymbol{\eta}^T(j)] = \delta_{ij}\mathbf{R}(i)$.

The information filter can be written as:

$$\mathbf{y}(k | k) = \mathbf{y}(k | k-1) + \mathbf{i}(k) \quad (25)$$

$$\mathbf{Y}(k | k) = \mathbf{Y}(k | k-1) + \mathbf{I}(k), \quad (26)$$

where

$$\mathbf{i}(k) = \mathbf{H}(k)\mathbf{R}^{-1}(k)\mathbf{z}(k) \quad (27)$$

is the information state contribution from the observation $\mathbf{z}(k)$ and

$$\mathbf{I}(k) = \mathbf{H}(k)\mathbf{R}^{-1}(k)\mathbf{H}^T(k) \quad (28)$$

is its associated information matrix. The predictions are given by:

$$\mathbf{y}(k | k-1) = \mathbf{Y}(k | k-1)\mathbf{F}(k)\mathbf{Y}^{-1}(k-1 | k-1)\mathbf{y}(k-1 | k-1) \quad (29)$$

and

$$\mathbf{Y}(k|k-1) = [\mathbf{F}(k)\mathbf{Y}^{-1}(k-1|k-1)\mathbf{F}^T(k) + \mathbf{Q}(k)]^{-1}. \quad (30)$$

The update stage has the following form:

$$\mathbf{y}_i(k|k) = \hat{\mathbf{y}}_i(k|k-1) + \sum_{j=1}^N \mathbf{i}_j(k) \quad (31)$$

$$\mathbf{Y}_i(k|k) = \hat{\mathbf{Y}}_i(k|k-1) + \sum_{j=1}^N \mathbf{I}_j(k), \quad (32)$$

where N is the total number external sensors.

The information filter has several advantages over the covariance form of the Kalman filter. It allows for the initialisation of the filter for the cases where \mathbf{P}_0^{-1} is singular. Furthermore, for multi-sensor systems, the computational requirement of the filter is less than those of the standard Kalman filter. The reason is that the information filter requires the inversion of the information matrix that is of the dimension of the state vector, while the standard form requires the inversion of the composite innovation covariance matrix which is of the dimension of the observation vector.

Also, as shown by equations 25 and 26, the filter only requires additions at the estimation (update) stage. This property can be exploited for efficient data fusion for systems with multiple sources of information. This will be the case where more than one external sensor is available to update the dead reckoning information. In our case the benefit are obtained updating the states in a sequential manner with each landmark detected.

Nonlinear Information Filter

The prediction and observation models for the vehicle under investigation are non-linear. For such system, a nonlinear information filter can be used. This filter is equivalent to the Extended Kalman Filter and linearises the nonlinear model around the nominal state to obtain the best linearised estimates for the nonlinear system. Consider a nonlinear system represented by

$$\mathbf{x}(k) = \mathbf{f}[k, \mathbf{x}(k-1)] + \omega(k) \quad (33)$$

with the observation model

$$\mathbf{z}(k) = \mathbf{h}[k, \mathbf{x}(k)] + \eta(k). \quad (34)$$

The information contribution from an observation for this case is again obtained from equations 27 and 28, substituting

$$\mathbf{H}(k) = \nabla_{\mathbf{x}} \mathbf{h}[k, \mathbf{x}(k|k)] \quad (35)$$

and replacing \mathbf{z} by

$$\mathbf{z}' = \mathbf{z} - (\mathbf{h}[k, \mathbf{x}(k|k-1)] - \nabla_{\mathbf{x}} \mathbf{h}[k, \mathbf{x}(k|k-1)]\mathbf{x}(k|k-1)) \quad (36)$$

where $\nabla_{\mathbf{x}} \mathbf{h}$ is the Jacobian of \mathbf{h} with respect to \mathbf{x} .

The nonlinear form of the information filter is identical to its linear form. However, for the calculation of the partial information state vector $\mathbf{i}_i(k)$ and its associated information matrix $\mathbf{I}_i(k)$, equations 35 and 36 must be used. The prediction equation 29 is replaced by

$$\mathbf{y}(k|k-1) = \mathbf{Y}(k|k-1)\mathbf{f}[k, \mathbf{x}(k-1|k-1)]. \quad (37)$$

and the inverse covariance is updated with:

$$\mathbf{Y}(k|k-1) = [\nabla f_x(k)\mathbf{Y}^{-1}(k-1|k-1)\nabla f_x^T(k) + \mathbf{Q}(k)]^{-1} \quad (38)$$

5 Results

The navigation system was tested with a utility vehicle retrofitted with the sensors described. The utility car used for the experiment is shown in Figure 7. The laser and the GPS antenna are mounted in front of the vehicle. A map of the testing site (landmarks positions) and a typical car trajectory is shown in Figure 8. The vehicle was driven at speed of up to 4 m/sec. The experimental runs were performed in the top level of the car park building of the university campus. This testing site was chosen to maximize the number of satellite in view. A Kinematic Glonass/GPS system of 1 cm accuracy was used to generate ground truth information. The “stars” in the map represent potential natural landmarks and the “circles” are the artificial reflective beacons. Although this environment is very rich with respect to the number of natural landmarks, the data association becomes very difficult since most of the landmarks are very close together. Under a small position error the navigation algorithm will not be able to associate the extracted features correctly. The inclusion of beacons becomes equivalent to the introduction of a different type of landmark that is validated at the sensor level. This will make the data association of the natural landmark possible with the potential of a significant reduction of the localization error.



Figure 7. Utility car used for the experiments.

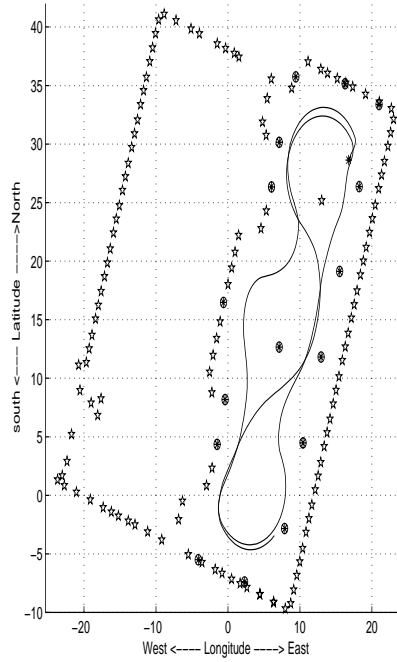


Figure 8 Landmark Positions and a typical trajectory (Latitude and Longitude in meters)

Figure 9 shows a typical laser frame with the vehicle positioned at (0,0). The lines indicate high intensity reflection and coincide with the reflective beacons.

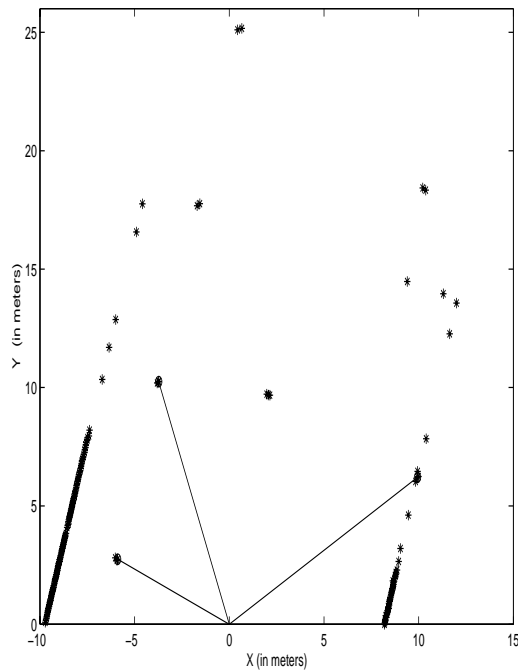


Figure 9 A typical laser frame

The data association is then performed considering the a-priori estimates and uncertainties in landmarks positions and the covariance of vehicle position and orientation.

Navigation using beacon at known locations

The first set of results corresponds to the localization algorithms using the reflective beacons at known locations. The final trajectory with the beacons used is presented in Figure 10.

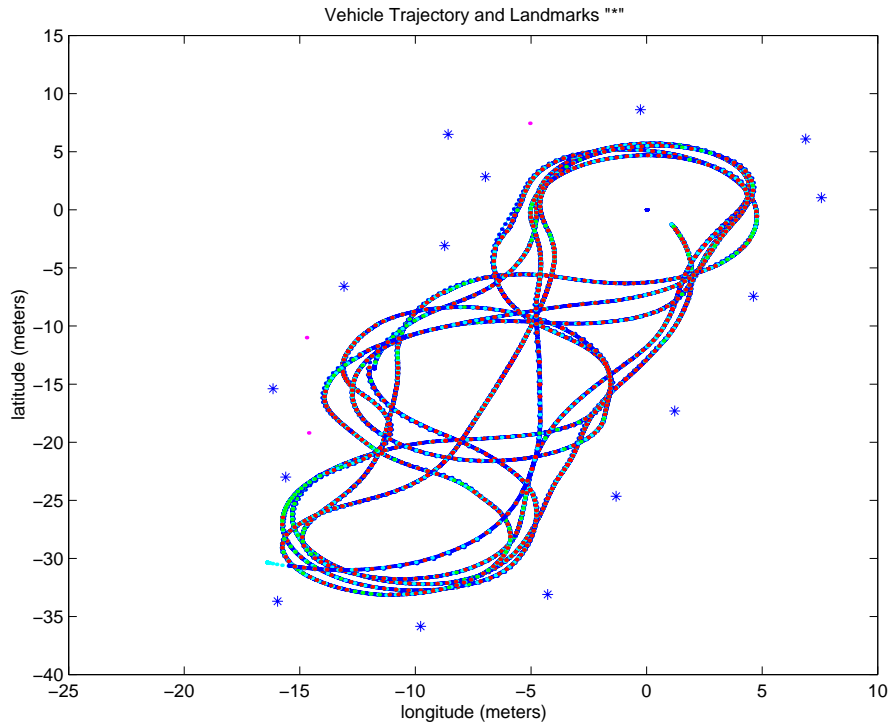


Figure 10. Final estimation using artificial landmarks

Figure 11 presents the 95 % confidence bounds of the estimated position of the vehicle, continuous line, with the true error, dotted line. It can be seen that most of the errors are bounded by the 95 % confidence bounds estimated by the filter. It is also important to note that the localizer is able to estimate the position of the vehicle with an error of approximate 6 centimetres. This is a very important achievement considering the systematic errors present in the surveying and detection of the landmarks and vehicle model errors.

A better representation of the uncertainty in estimation process can be obtained considering the complete covariance sub-matrix P_{xy} . Figure 12 presents the uncertainty in x and y considering the off diagonal terms of P_{xy} . The 2-D standard deviation errors are presented with the ground truth provided by the GPS position information. It can be noted that the error region reduces abruptly when the number of observations increase, coordinate (-8.4,-1), that is increasing the number of beacons used in the update stage. This plot also presents the evolution of the magnitude of the uncertainty regions when no observations are obtained. This is due to the cumulative effects of the model uncertainty.

Finally, a subset of the trajectory presented in Figure 13 when the vehicle is turning, coordinate (-11,-33). At this moment the model is expected to have some systematic errors due to slip and steering nonlinearities. It can be seen that a strong correction of few centimetres is performed by the filter in the update stage. This can be reduced using a larger number of beacons or with the addition of artificial landmarks as will be shown later.

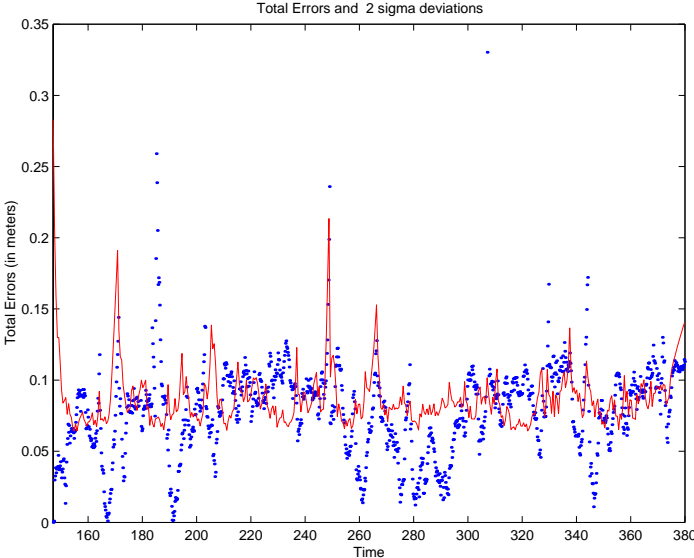


Figure 11 Standard deviation with beacons

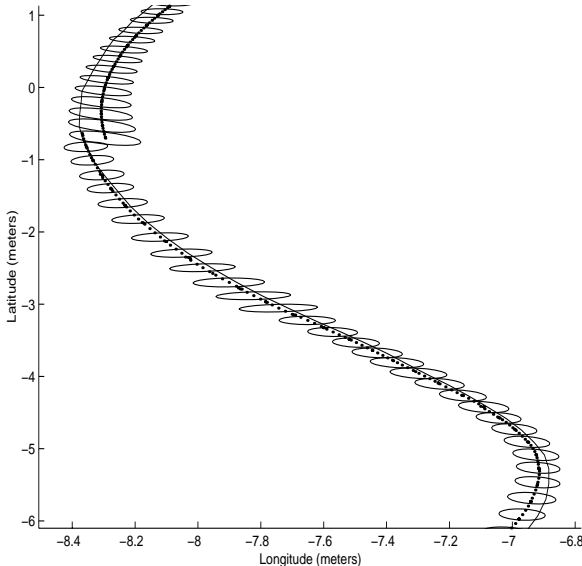


Figure 12, Position estimates and variances

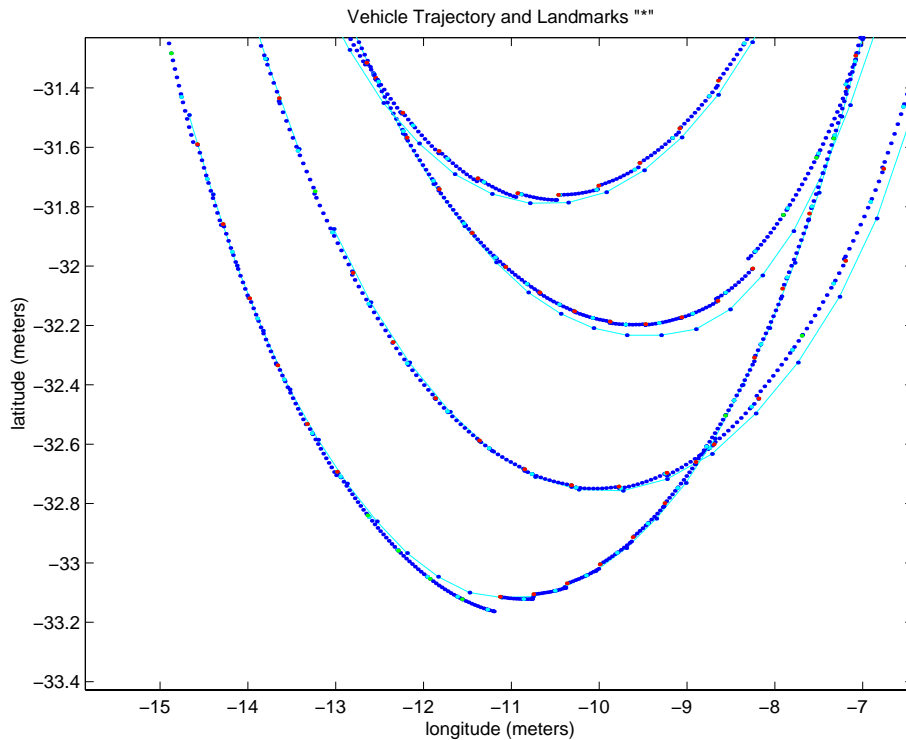


Figure 13 Enhanced Trajectory.

Navigation using SLAM with artificial beacons

The second experimental results correspond to SLAM using only beacons. In this case it is not necessary to survey the position of the beacons. This information is obtained while the vehicle navigates. The system builds a map of the environment and localize itself. The accuracy of this map is determined by the initial uncertainty of the vehicle and the quality of the combination of dead reckoning and external sensors. In this experimental results an initial uncertain of 10 cm in coordinates x and y was assumed. Figure 14 shows the initial part of the experimental run with only few beacons detected. The actual trajectory is plotted as a continuous line while the total GPS trajectory is drawn as a dotted line. Figure 15 presents the absolute error and the predicted standard deviation (2σ bounds, 95% confidence bounds). These plots show that the bounds are consistent with the actual error. It is also important to remark that the uncertainty in position does not reduce below the initial uncertainty. This is expected since the laser information is obtained relative to the vehicle position. The only way the uncertainty can be reduced is by incorporating additional information that is not correlated to the vehicle position, such as GPS position information or recognizing a beacon with known position.

The laser range innovation sequence can be seen in Figure 16 . It remains white and validates the assumed statistic for the model and sensors. The landmark covariance estimation is shown in Figure 17 . This figure presents the variance of position x and y and the estimated uncertainty of a selected group of landmarks. The ones with oscillatory behaviour correspond to the uncertainty of the vehicle. This is expected since no external absolute information is incorporated by the filter. The original uncertainty of a new landmark will be a function of the actual vehicle uncertainty and sensor noise. It can be seen that the landmark once created are started with different initial covariances. This value is a function of the current vehicle uncertainty and the quality of the observation. It then decrease with time to a value that will not be smaller than the initial uncertainty of the vehicle. It can also be appreciated from this plot that the due to the correlation of the map all landmarks are being updated all the time.

Finally Figure 18 shows that since we are still using the same number of beacons, there is no improvement with respect to the smoothness of the updates when compared to the absolute navigation algorithm. There is a still a strong correction due to the failure of the vehicle's model, coordinate (-11,-33).

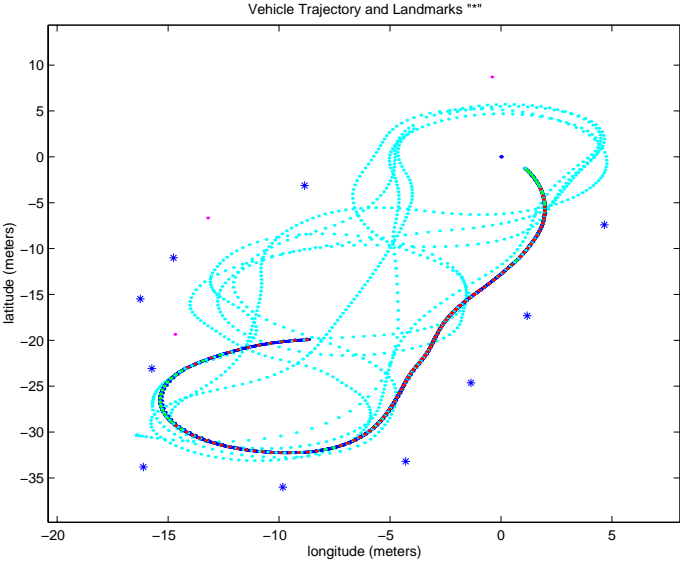


Figure 14. Initial part of the trajectory using SLAM with beacons

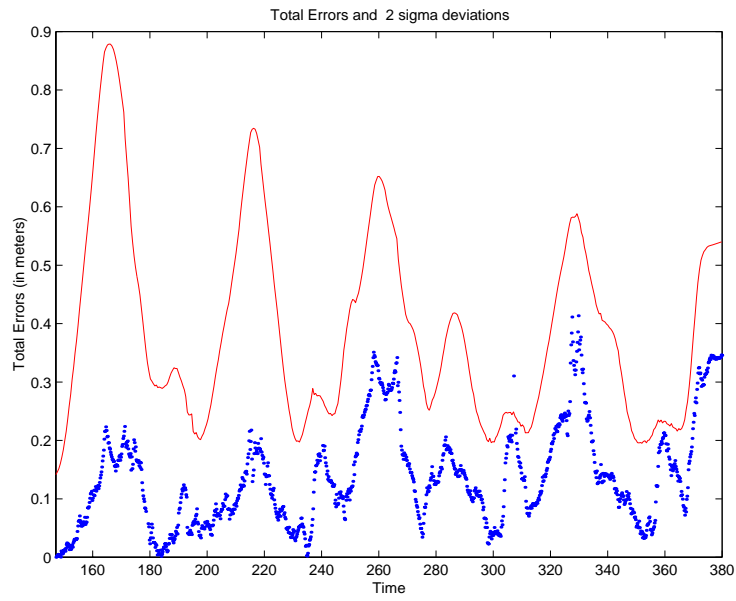


Figure 15 Absolute position error and standard deviation.

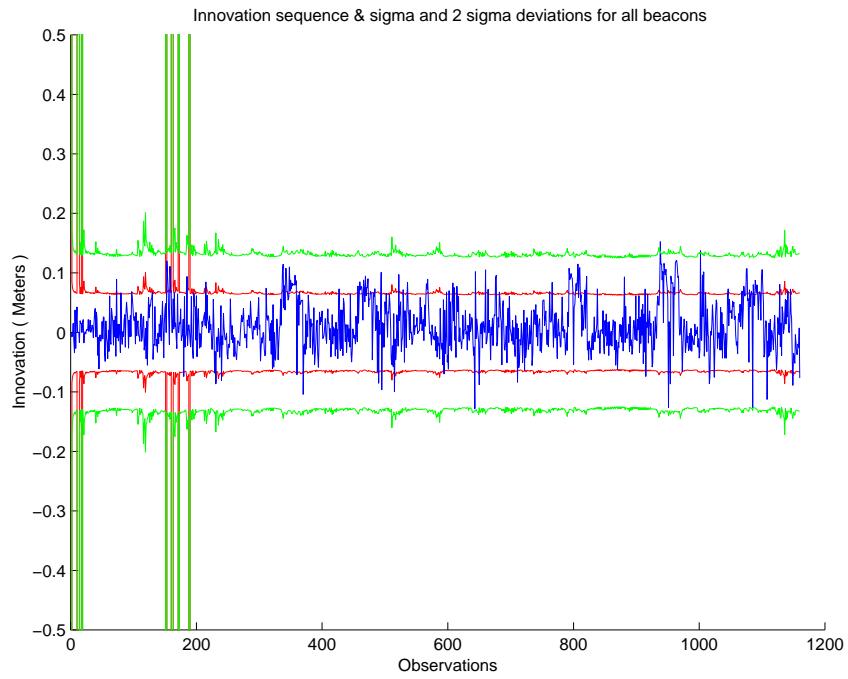


Figure 16 Innovation sequence SLAM with beacons

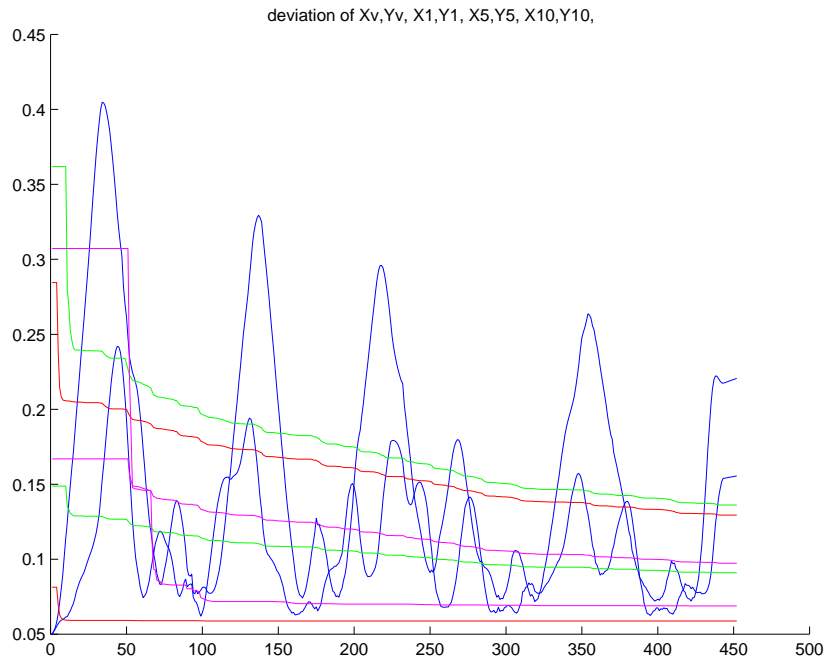


Figure 17 Estimated deviation of position and beacons

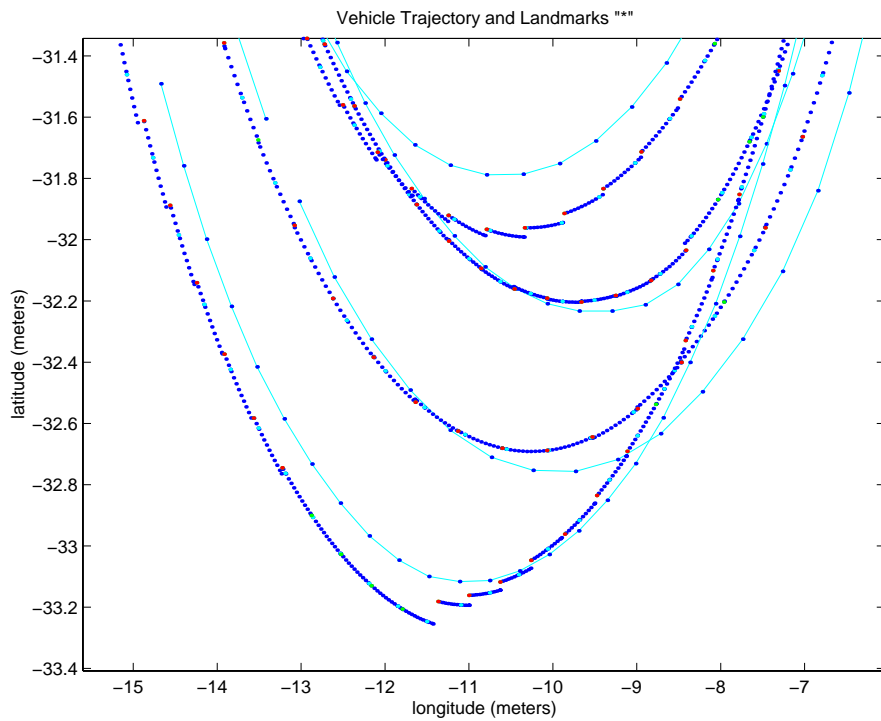


Figure 18 Enhanced Trajectory

Navigation using SLAM with Natural Features

The final experimental results correspond to SLAM using all the features available in the environment. In this case it is not required to modify the infrastructure of the environment with the addition of beacons. The most relevant navigation features are obtained while the vehicle navigates. The vehicle builds a navigation map of the environment, maintains it and localizes itself. The accuracy of this map is determined by the initial uncertainty of the vehicle and the quality of the combination of dead reckoning and external sensors installed in the vehicle and frequency of external observations. In this experimental results an initial uncertain of 10 cm in coordinates x and y was also assumed. Figure 19 shows the initial part of the experimental run while the system is still incorporating new landmarks. The actual trajectory is drawn with a continuous line while the total GPS trajectory is plot as a dotted line. Figure 20 presents the absolute error with the predicted standard deviation (2σ bounds, 95 % confidence bounds). These plots show that the bounds obtained using all landmarks are consistent with the actual errors. It is also important to remark that the uncertainty in position become significantly smaller than the SLAM with beacons only. This is due to a larger number of landmarks that incorporate more information to the filter. The uncertainty does not become smaller than the initial uncertain. This is expected since the laser information is obtained relative to the vehicle position.

The laser range innovation sequence can be seen in Figure 21 . It remains white and validates the assumed statistic for the model and sensors. The landmark identification covariance is shown in Figure 22 . This figure presents the variance of position x and y with the uncertainty of some selected landmarks. The ones with oscillatory behaviour correspond to the uncertainty of the vehicle. The landmarks are originally incorporated with an initial uncertainty function of vehicle and sensor covariances. The positions are then updated and its uncertainties are reduced as shown in the Figure. It can also be appreciated from this plot that the due to the correlation between landmarks and landmarks and vehicle's states, the landmark are being updated all the time even if they are not being observed at the present time.

Finally Figure 23 shows that since we are using a larger number of features there is a considerable improvement with respect to the smoothness of the updates. This trajectory can be compared to Figures 13 and 18 where a much smaller number of landmarks are being used. This can be important for vehicle control purposes since less demand will be imposed on the control and actuators.

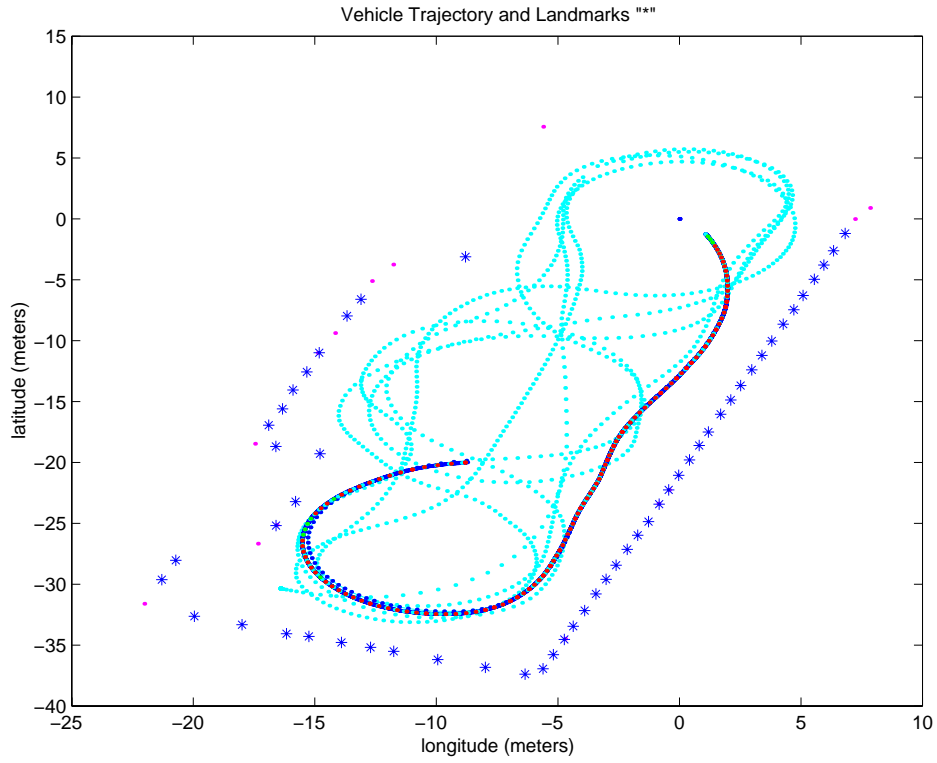


Figure 19. Initial part of the trajectory using SLAM with natural features and beacons

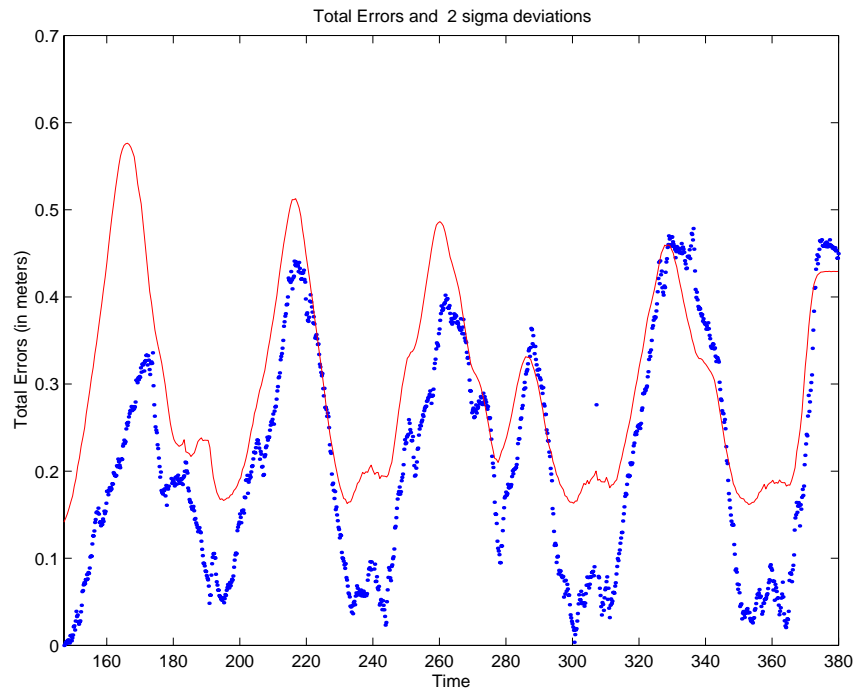


Figure 20 Absolute position error and standard deviation.

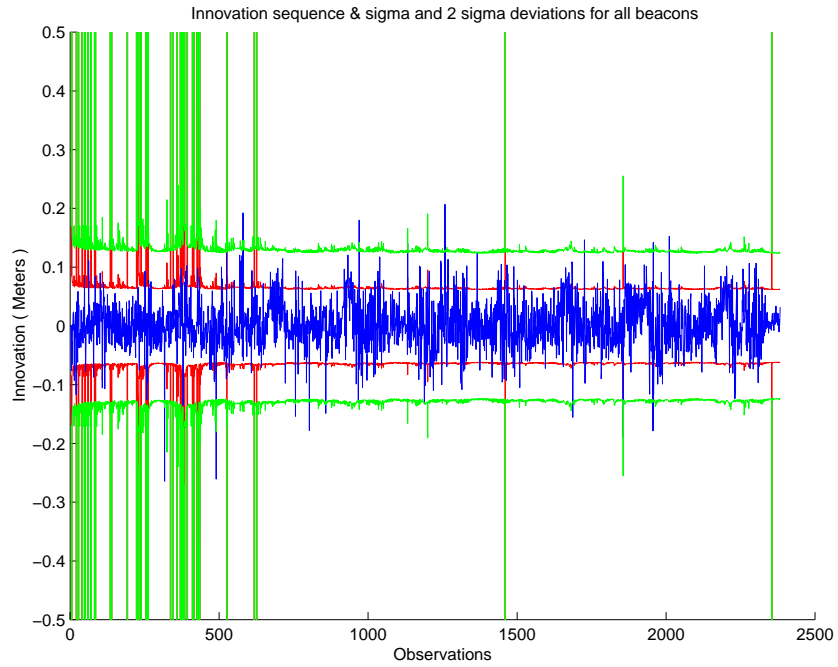


Figure 21 Innovation sequence SLAM with natural features

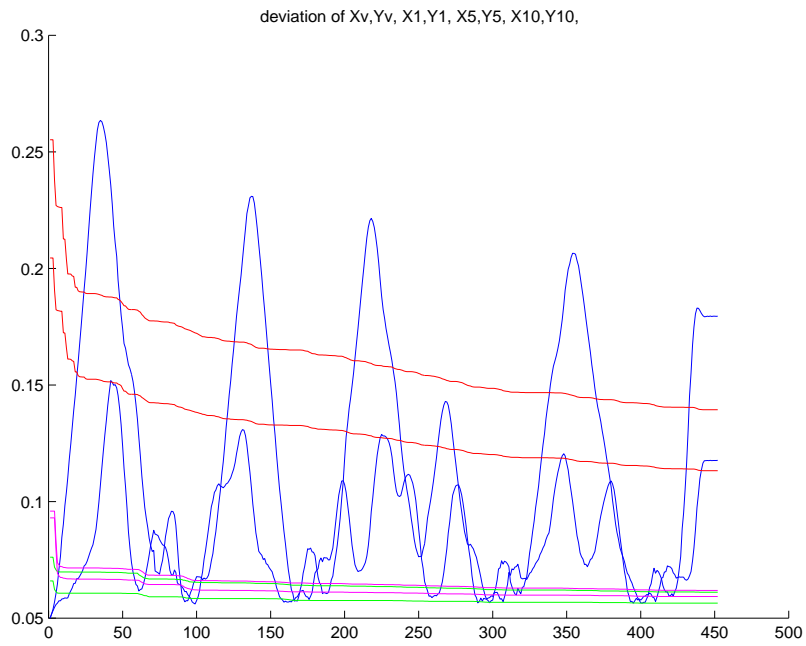


Figure 22 Estimated deviation of position and selected features

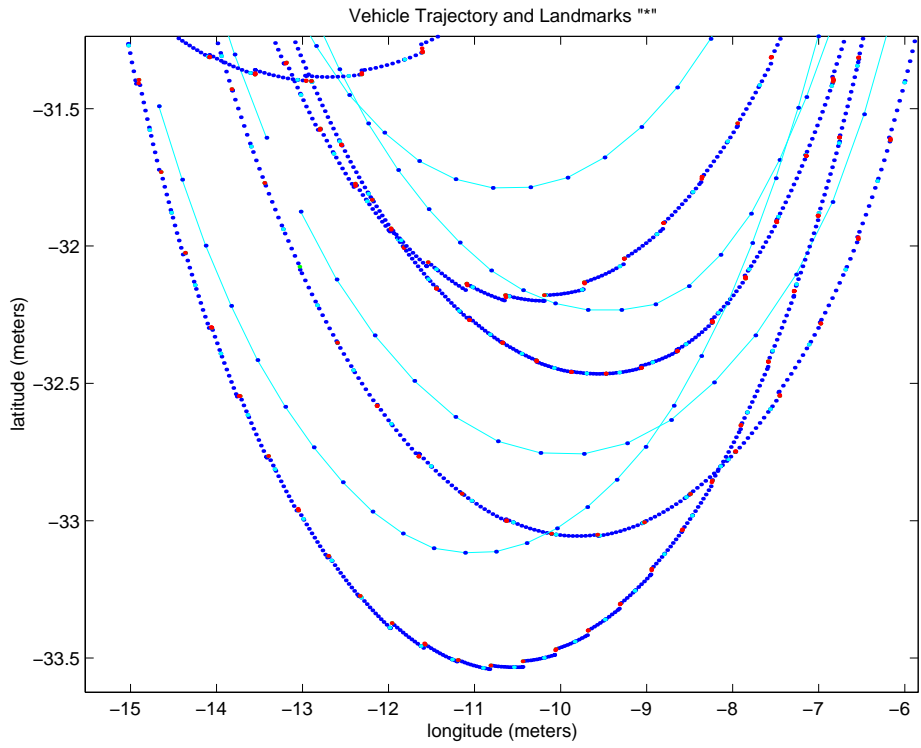


Figure 23 Enhanced Trajectory

6 Conclusion

This work presented the implementation of different types of high accuracy navigation algorithms for outdoor and indoor applications. A characterization of a range/bearing/intensity laser is also presented. This task is essential to design beacons for a particular navigation environments. The modelling aspect and the design of navigation algorithms are presented with an implementation based on the Information Filter. This approach becomes more attractive than the standard Kalman filter form for the case where a large number of observation are present. Sequential processing of the laser landmark information becomes much more efficient since it does not require the re-evaluation of the Kalman gain matrix.

The modelling aspect has also been extended to consider Simultaneous Localization and Map building (SLAM). A full implementation of SLAM using beacons is also presented. This is an important contribution since it does not require any surveying of the beacons. The actual results have shown that the algorithm can deliver an accuracy in accordance to the initial uncertainty of the vehicle. It is important to remark that the maps obtained are relative to the initial position and orientation of the vehicle. In many application this will be all that is needed to accomplish a certain task. In case the absolute position is required to use external information such as GPS, then the uncertainty needs to be incorporated as shown in these two examples. It was also demonstrated that the algorithm successful build and maintain a map for long runs. This experimental results presented a 3 km run and the algorithm remains stable. In fact after revisiting the old landmarks the problem transform to the standard navigation algorithm with known beacon position.

Finally SLAM considering all natural features is presented. It is demonstrated that it is not always necessary to use specially designed beacon for navigation purposes. In fact in this case the only requirement for the algorithm was the initial position and uncertainty of the vehicle. With only this information the algorithm was able to estimate the position of the vehicle with cm accuracy. It is important to remarks that although in this case the beacons were not required, they can be of fundamental importance for the data association problem in cases were the distance between landmarks is smaller than the position error build-up that will eventually appear when exploring new areas. This will always be a function of the particular application.

Although the Information filter implementation presented in this paper is efficient for the navigation problem it may be computationally expensive for the SLAM in the case where the number of landmarks become large. We are currently investigating more efficient implementations of this algorithm taking into consideration the sparseness of the matrix involved in SLAM.

References

- [1] Nebot E., Durrant-Whyte H., "High Integrity Navigation Architecture for Outdoor Autonomous Vehicles", Journal of Robotics and Autonomous Systems, Vol. 26, February 1999, p 81-97.
- [2] Sukkarieh S., Nebot E., Durrant-Whyte H., "A High Integrity IMU/GPS Navigation Loop for Autonomous Land Vehicle applications", IEEE Transaction on Robotics and Automation, June 1999, p 572-578.
- [3] Scheduling S., Dissanayake, Nebot E., Durrant-Whyte H., "An Experiment in Autonomous Navigation of an Underground Mining Vehicle", IEEE Transaction on Robotics and Automation, Vol. 15, No 1, February 1999, p 85-95.
- [4] Nebot E., "Sensors used for autonomous navigation", Advances in Intelligent Autonomous Systems, Chapter 7, pp. 135-156, ISBN 0-7923-5580-6, March 1999, Kluwer Academic Publishers, Dordrecht .

- [5] Elfes A., "Sonar based real-world mapping navigation", IEEE J. Robotics Automation, 3(3), p 249-265, 1987.
- [6] Drocourt C., Delahoche L., Pegard C., Clerentin A., "Mobile Robot Localization Based on an Omnidirectional Stereoscopic Vision Perception System", Proc. of the 1999 IEEE Conference on Robotics and Automation, Detroit, USA, pp 1329-1334.
- [7] Clark S., H. Durrant-Whyte, "Autonomous land vehicle navigation using millimeter wave radar", Int. Proc. of the IEEE International conference of Robotic and Automation, Belgium, May 1998, p 3697-3792.
- [8] Durrant-Whyte H., "An Autonomous Guided Vehicle for Cargo Handling Applications", Int. Journal of Robotics Research, 15(5): 407-441, 1996.
- [9] Clark S., Dissanayake G., "Simultaneous Localisation and Map Building Using Millimetre Wave Radar to Extract Natural Features", Proc. of the 1998 IEEE Conference on Robotics and Automation, Detroit, USA 1999, pp 1316-1321.
- [10] Madhavan, R.; Dissanayake, M.; Durrant-Whyte, H.F.; "Autonomous Underground Navigation of an LHD using a combined ICP-EKF approach" IEEE Conference on Robotics and Automation Proceedings of the 1998 Belgium, p 3703-3708
- [11] Jensfelt P., Christensen H., "Laser Based Pose Tracking", Proc. of the 1999 IEEE Conference on Robotics and Automation, Detroit, USA, pp 2994-2998.
- [12] Castellanos J., Martinez J., Neira J., Tardos J., "Simultaneous Map Building and Localization for Mobile Robots: A multisensor Fusion Approach", Proc. of the 1998 IEEE Conference on Robotics and Automation, p 1244-1249.
- [13] Perez J., Castellanos J., Montiel J., Neira J., Tardos J., "Continuous Mobile Robot Localization: Vision vs. Laser", Proc. Of the 1999 IEEE Conference on Robotics and Automation, p 2917-2923.
- [14] Smith C., Feder J., Leonard J., "Multiple Target Tracking with navigation Uncertainty", International conference on decision and Control, December 1999.